Novel Hybrid Propagation Model inside Tunnels

Ke Guan*, Zhangdui Zhong*, Bo Ai* and Cesar Briso-Rodríguez†
*State Key Laboratory of Rail Traffic Control and Safety
Beijing Jiaotong University, 100044, Beijing, China
†Escuela Universitaria de Ingeniería Técnica de Telecomunicación
Universidad Politécnica de Madrid, 28031, Madrid, Spain
E-mail: myecone@hotmail.com

***Abstract*—The propagation situations inside tunnels vary with the distance between transmitter and receiver, as well as the relative size of the users. This paper presents a novel hybrid propagation model covering three propagation mechanisms with two types of users. In the first case, the users are relatively small in size compared with the tunnel. The entire process is interpreted by combining the free space propagation model and the limited multi-mode propagation model. In the second case, for relatively large users , the free space propagation can be replaced by the near shadowing effect to some extent or totally. Hence, the whole procedure is described by coupling the statistical model in the near shadowing zone, the free space model, and the limited multi-mode model. Two groups of measurements are employed to validate the model. The results show good agreement and, therefore, the model supports an effective way to predict the propagation situation inside tunnels for different types of users.**

***Index Terms*—modeling; propagation; tunnel**

I. Introduction

To give the answer to the growing demand for high-performance radio communication systems operating in tunnels, many investigators have performed simulations and measurements of wave propagation in the last four decades.

It is known that ray tracing [1] [2], modal analysis [3] [4], empirical models [5], and vector parabolic equation (VPE) [6] are the main methods of propagation modeling. However, each of them has own pros and cons. The ray tracing method provides accurate prediction, but with too complex computation and extremely rigorous environment information. Empirical models are easy to use, but the accuracy is not excellent. Moreover, due to the dependency on the measurement in some certain environments, they would be less useful when the environment changes. Modal analysis supplies prediction with higher accuracy when the receiver is far away from the transmitter, but lower accuracy in the adjacent region of the transmitter. The model based on VPE involves both loss and fading characteristics and can work in straight and curved tunnels with arbitrary cross section. Nevertheless, VPE approximation does not accurately model high-order modes and corresponding rapid fluctuations [6].

This work is supported by the NNSF of China under Grant 60830001, Program for New Century Excellent Talents in University under Grant NCET-09-0206, Beijing NSF 4112048, the Key Project of State Key Lab. of Rail Traffic Control and Safety under Grant RCS2008ZZ006, the Fundamental Research Funds for the Central Universities under Grant 2010JBZ008 and the State Key Lab. of Rail Traffic Control and Safety (Contract No. RCS2008ZT005, No. RCS2010ZT012 and No. RCS2010K008), Beijing Jiaotong University.

Hence, a single modeling technique is always sensitive to certain propagation mechanisms or characteristics. Since the propagation inside tunnels includes various mechanisms, it is highly desired to present a hybrid propagation model integrating advantages of different techniques.

Generally speaking, LOS (line-of-sight) between transmitter and receiver can always be maximally kept in system design; however, in realistic situations, since the antennas cannot always be on the top of the user, for instance, the referenced antenna configuration on-train in Madrid subway [7], LOS can be blocked by the user itself when passing in front of the transmitter. Thus, we separate the users into two categories and model the propagation corresponding to each one. The users whose size is far less than the tunnel size, not possibly blocking LOS, such as pedestrians, light cars in road tunnels, trains in high speed railway tunnels, etc., are named relatively small-size users. The users whose size is close to the tunnel size, e.g. trains in subway tunnels, large trucks in road tunnels, are defined as relatively large-size users.

II. Propagation mechanisms inside tunnels

Along with the increase of the distance between receiver and transmitter, for the relatively small-size users, the free space propagation mechanism comes first, the multi-mode waveguide effect establishes later. For relatively large-size users, the first mechanism is near shadowing. Then, the free space propagation occurs before the waveguide propagation if LOS recovering is earlier than the end of the free space propagation. Otherwise, the multi-mode waveguide propagation is behind the near shadowing effect, no free space propagation exists.

A. Free space propagation mechanism

When the receiver stays in the adjacent region of the transmitter, the first Fresnel zone is not large enough to touch any wall or obstructions, so the diffraction effects may be neglected. Meanwhile, the angles of incidence from the ray to the wall are high leading to high attenuation of reflected rays. Furthermore, the path difference between the direct ray and reflected rays may cause additional attenuation. All these lead to the result that the already weak reflected rays are further weakened. As a consequence, only the direct ray significantly contributes to the strength of the received signal. Thus, the propagation follows free space mechanism. Subsequently, when the receiver is moving away from the

978-1-4673-0990-5/12/$31.00 ©2012 IEEE

transmitter, at one point where the first Fresnel zone will touch the wall, then the reflection starts to occur inside the first Fresnel zone and effectively reinforces the signal strength at the receiver. This means the end of the free space propagation zone. The location of this point is modeled in [8].

B. Multi-mode waveguide mechanism

After the point where the first Fresnel zone is tangent to the walls or obstructions, the first Fresnel zone becomes no longer clear along with its own expansion. This can be treated as the process that the walls penetrate the first Fresnel zone and generate many effective reflected rays, which are regarded as modes in waveguide theory. Hence, the propagation can be calculated by the superposition of multiple modes.

C. Near shadowing mechanism

In some realistic vehicular cases, the relatively large-size users can block LOS by themselves when approaching and passing the transmitter. This very important effect has been observed that when the train is in front of the transmitter the received signal power of referenced configured antennas on train suffers a strong attenuation and propagation has strong multi-paths [7]. This phenomenon is named near shadowing; the corresponding area is referred to as near shadowing zone.

III. Novel hybrid propagation model

By combining the advantages of various modeling methods, a novel hybrid propagation model is proposed. Unlike existing hybrid models [5] [9], this one supplements the near shadowing zone and supports various structures for different users.

A. Propagation loss in the free space propagation zone

In the adjacent region of the transmitter antenna, the propagation characteristics follow the rule of the free space propagation. Hence, this region is named as the free space propagation zone. A similar naming method is used in [10].

The loss in this segment follows the free space model [11]

$$L_{R_{FS}}\left(dB\right) = -10\log_{10}\left[\frac{\lambda^2}{\left(4\pi\right)^2\left|z_r - z_t\right|^2}\right] \tag{1}$$

where $|z_r - z_t|$ is the distance between the transmitter and the receiver in metres, and λ is the signal wavelength.

B. Statistical modeling in the near shadowing zone

This zone was discovered in the measurements reported in [7]. Fig. 1 demonstrates the whole process of the near shadowing phenomenon. When the distance between train and transmitter is shorter than the length of the train, the signal is blocked by the carriage so that the near shadowing effect occurs. When the train is running out of this region, the coverage recovers. The region lasts two times the length of the train (in the measurement [7] it is (2×60 m)) and this situation is especially important in subway where normally the tunnels are narrow.

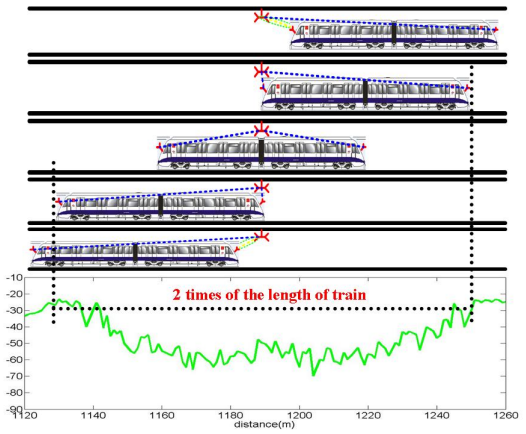

Fig. 1. Sketch of the mechanism of the near shadowing zone in tunnels.

Note that although the measurement is performed at 2.4 GHz, it still represents the character of some realistic advanced radio communication systems, such as TETRA (Terrestrial Trunked Radio), CBTC (Communication-Based Train Control System), etc. In these, the antennas are directive and in narrow tunnels with pipes and cables on the wall it is impossible to get LOS with the transmitter when the train is passing, even if the antennas are located in the upper part of the train.

Denote the maximum near shadowing loss when there is no LOS between the transmitter and the receiver by $NL_{\max}$. Since such NLOS situation results from the block effect of the carriage, it is obvious that the following relation exists: the bigger the train, the easier LOS is blocked; the bigger the tunnel, the harder LOS is blocked. Thus, $NL_{\max}$ is proportional to the height and width of the section of the train, but inversely proportional to the height and width of the section of the tunnel. With this analysis, by using the principle of least-squares curve fitting on the measured data in [12], $NL_{\max}$ can be modeled as:

$$NL_{\max} = 16.1 \times \frac{h}{H} + 31.2 \times \frac{w}{W} \tag{2}$$

where w and h are the width and height of the cross section of the train, respectively; W and H are the width and height of the cross section of the tunnel, respectively.

By involving the shadow fading parameter and using the point slope form, the propagation model in the near shadowing zone is expressed by

$$L_{R_{NS}} = \frac{PL_l - (NL_{\max} + PL_0)}{l_{near}}\left|z_r - z_t\right| + (NL_{\max} + PL_0) + X_\sigma \tag{3}$$

where $|z_r - z_t|$ is the distance between transmitting antenna and receiving antenna; PL_l represents the path loss at the point where the distance is the length of the train; l_{near} is the half length of the near shadowing zone, always equaling the length of vehicle; PL_0 is the path loss under LOS condition when the distance between train and transmitter is 0 m, which can be calculated by the free space propagation model. X_σ represents a log-normal distribution with standard deviation σ. The values of this parameter have been exhibited in [7] for wide tunnel and narrow tunnel, respectively.

C. Limited multi-mode modeling for waveguide propagation

No matter the user is relatively small in size or large, the multi-mode waveguide propagation occurs when the receiver is not close to the transmitter. Compared with [13], the novel model clarifies the limitation of the excited modes and introduces new calibrating factors.

1) The first stage: parameterization of the environment: Although the arched tunnel is the most common type, the field variation inside arched tunnels and circular tunnels can be predicted with sufficient accuracy by assuming a rectangular tunnel [14]. Hence, the tunnel cross section is treated as an equivalent rectangle. The following parameters are supplied:

- Coordinate system: Cartesian coordinate system, with its origin located at an angle of the rectangle tunnel.
- Geometric dimension: width: W; height: H.
- Operating frequency: central frequency of the signal: f_0; central angular frequency: $\omega_0 = 2\pi f_0$.
- Electrical parameters: relative permittivity for vertical/horizontal walls and the air in the tunnel: ε_v, ε_h and ε_a; conductivity for vertical/horizontal walls and the air in the tunnel: σ_v, σ_h and σ_a; permeability for vertical/horizontal walls and the air in the tunnel: μ_0; permittivity in vacuum space: ε_0; the complex electrical parameters of the tunnel for vertical/horizontal walls and the air in the tunnel: $\varepsilon_v^* = \varepsilon_0\varepsilon_v + \frac{\sigma_v}{i\omega_0}$, $\varepsilon_h^* = \varepsilon_0\varepsilon_h + \frac{\sigma_h}{i\omega_0}$ and $\varepsilon_a^* = \varepsilon_0\varepsilon_a + \frac{\sigma_a}{i\omega_0}$.
- Relative electrical parameters: $\varepsilon_{rv}^* = \frac{\varepsilon_v^*}{\varepsilon_a^*}$; $\varepsilon_{rh}^* = \frac{\varepsilon_h^*}{\varepsilon_a^*}$.

2) The second stage: quantification of the excited modes: Quantity and modes of guide waves have to be determined. From the theoretical point of view, due to the size of the tunnels, the cutoff frequency of the fundamental modes is very low; therefore, a wide range of E_{mn} hybrid modes exist in the tunnel when the radio communication system is in UHF. However, the number of E_{mn} waves is not infinite. Thus, ascertaining the quantity and mode of all the E_{mn} guide waves excited by the source is crucial to the propagation model.

According to modal theory, the cutoff wave number for a rectangular tunnel can be roughly estimated as [15]:

$$k_c = \sqrt{\left(\frac{m\pi}{W}\right)^2 + \left(\frac{n\pi}{H}\right)^2} \tag{4}$$

where m and n are approximate numbers of half-wave loops in the horizontal and vertical directions. The condition of the signal propagating in a tunnel is:

$$\sqrt{k^2 - k_c^2} > 0 \tag{5}$$

where k is the wave number in the tunnel space given by $k = \omega_0\sqrt{\mu_0\varepsilon_0\varepsilon_a}$. The inequation indicates that arbitrary mode E_{mn} can transmit in a tunnel if (m, n) satisfies:

$$\sqrt{\left(\frac{m\pi}{W}\right)^2 + \left(\frac{n\pi}{H}\right)^2} < \omega_0\sqrt{\mu_0\varepsilon_0\varepsilon_a} \tag{6}$$

In order to deduce all the modes existing in a tunnel, the inequation above necessitates to be solved. Firstly, $m_{\max}$, the maximum of m, can be obtained by rounding the result of the equation towards minus infinity:

$$m_{\max} = \left\lfloor \frac{W}{H}\sqrt{4H^2 f_0^2 \mu_0\varepsilon_0\varepsilon_a - 1} \right\rfloor \tag{7}$$

Then, all the n corresponding to each $m \in [1, m_{Max}]$ can be gained by substituting each m into (6) in turn:

$$\begin{aligned} &1 \le n_{ij} \le \left\lfloor \tfrac{H}{W}\sqrt{4W^2 f_0^2 \mu_0\varepsilon_0\varepsilon_a - m_i^2} \right\rfloor, \\ &i \in [1, m_{\max}], j \in \left[1, \left\lfloor \tfrac{H}{W}\sqrt{4W^2 f_0^2 \mu_0\varepsilon_0\varepsilon_a - m_i^2} \right\rfloor\right] \end{aligned} \tag{8}$$

Here, all the E_{mn} have been determined. Note that the quantity and mode of all the guide waves are ascertained both by the working frequency and the dimension of tunnel. Fig. 2 shows the calculated results of all the E_{mn} excited by the source at 2400 MHz in a wide tunnel (9.6 m×6.1 m) and a narrow tunnel (4.8 m×5.3 m), respectively.

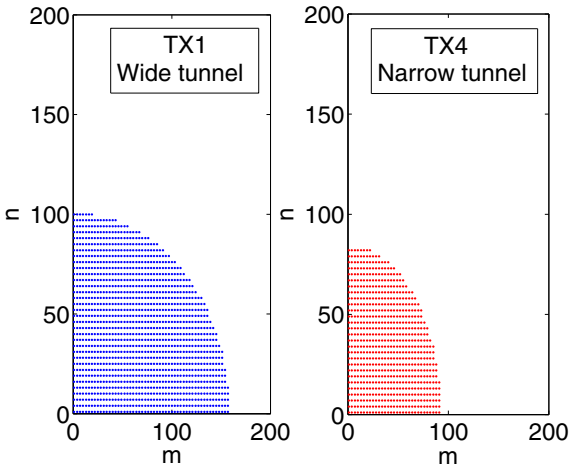

Fig. 2. E_{mn} excited by the source at 2400 MHz in wide tunnel (9.6 m×6.1 m) and narrow tunnel (4.8 m×5.3 m).

3) The third stage: general type of the field: The general type of field at any position $(x, y, |z_r - z_t|)$ inside tunnels is deduced. In modal theory, the propagation of E_{mn} waves in tunnels is regarded as the superposition of multiple modes with different field distribution and attenuation coefficients. Thus, by solving the Maxwell's equations, the field of each mode can be obtained in the form of eigenfunctions [16]:

$$E_{m,n}^{eign}(x, y) = \sin\left(\frac{m\pi}{W}x + \phi_x\right).\cos\left(\frac{n\pi}{H}y + \phi_y\right) \tag{9}$$

where $\phi_x = 0$ if m is even; $\phi_x = \frac{\pi}{2}$ if m is odd; $\phi_y = 0$ if n is odd; $\phi_y = \frac{\pi}{2}$ if n is even.

By considering the quantity of guide waves, the field can be expressed by summing up the field of limited excited modes:

$$\begin{aligned} &E^{Rx}(x, y, |z_r - z_t|) = \\ &\sum_{m=1}^{\left\lfloor \frac{W}{H}\sqrt{4H^2 f_0^2 \mu_0\varepsilon_0\varepsilon_a - 1} \right\rfloor} \sum_{n=1}^{\left\lfloor \frac{H}{W}\sqrt{4W^2 f_0^2 \mu_0\varepsilon_0\varepsilon_a - m^2} \right\rfloor} \\ &\rho_{mn} \cdot E_{m,n}^{eign}(x, y) \cdot e^{-(\alpha_{mn} + i\beta_{mn})\cdot|z_r - z_t|} \end{aligned} \tag{10}$$

where ρ_{mn} is the mode intensity on the excitation plane; α_{mn} and β_{mn} are the attenuation coefficient and the phase-shift

coefficient, respectively, given by [3][16]:

$$\alpha_{mn} = \frac{2}{W}\left(\frac{m\pi}{Wk}\right)^2 \mathrm{Re}\frac{\varepsilon_{rv}^*}{\sqrt{\varepsilon_{rv}^* - 1}} + \frac{2}{H}\left(\frac{n\pi}{Hk}\right)^2 \mathrm{Re}\frac{1}{\sqrt{\varepsilon_{rh}^* - 1}} \tag{11}$$

$$\beta_{mn} = \sqrt{k^2 - \left(\frac{m\pi}{W}\right)^2 - \left(\frac{n\pi}{H}\right)^2} \tag{12}$$

4) The fourth stage: mode intensity on the excitation plane: The mode matching technique is utilized to solve the mode intensity in the excitation plane: ρ_{mn}. In [13], the intensity of each mode in the excitation plane is deduced by a mode matching technique which converts the ray sum in the ray tracing model to the sum of complex modes in the cross-section of excitation. [13] gave the mode intensity in the excitation plane ρ_{mn}:

$$\rho_{mn} = \sum_{m=1}^{\infty}\sum_{n=1}^{\infty} \frac{4E_0\pi}{WH\sqrt{1-\left(\frac{m\pi}{Wk}\right)^2-\left(\frac{n\pi}{Hk}\right)^2}} \sin\left(\frac{m\pi}{W}x_0 + \phi_x\right)\cos\left(\frac{n\pi}{H}y_0 + \phi_y\right) \tag{13}$$

By substituting (13) into (10), the propagation of E_{mn} waves in tunnels can be ascertained. Fig. 3 illustrates the power distribution among all the excited modes at different distances along the tunnel. This result is calculated by the limited multi-mode model at 2400 MHz in (9.6 m×6.1 m) tunnel. As shown in Fig. 3, higher order modes are dominant near the transmitter but are quickly attenuated along with the increase of the distance, then only the fundamental mode propagates.

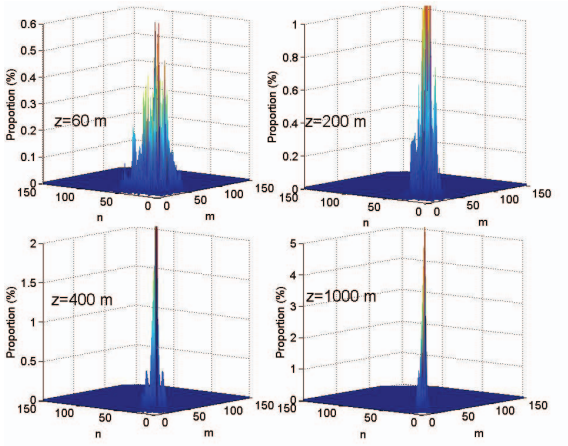

Fig. 3. Calculated power distribution among all the modes at different distances along the tunnel.

5) The fifth stage: supplementation of modifying factors: Since the approximation from an arched tunnel to a rectangular waveguide leads to certain deviation, two modifying factors are utilized. The first one is the tilt loss [17]:

$$L_{tilt}\left(|z_r - z_t|\right)[dB] = \frac{17.372\pi^2\theta^2}{\lambda}|z_r - z_t| \tag{14}$$

where θ is the root-mean-square tilt. The other one is the roughness loss which is calculated by [17]:

$$L_{roughness}\left(|z_r - z_t|\right)[dB] = 8.686\pi^2\gamma^2\lambda\left(\frac{1}{W^4} + \frac{1}{H^4}\right)|z_r - z_t| \tag{15}$$

where γ is the root-mean-square roughness.

6) The final stage: entire multi-mode propagation model: By substituting (13) into (9) and considering (14) and (15), the propagation loss at the coordinate $(x, y, |z_r - z_t|)$ can be analytically calculated by:

$$L_{R_{MW}} = L_{tilt}\left(|z_r - z_t|\right)[dB] + L_{roughness}\left(|z_r - z_t|\right)[dB] - 20\lg\left(\frac{1}{E_0}E^{Rx}\left(x, y, |z_r - z_t|\right)\right) - G_t\,[dB] - G_r\,[dB] \tag{16}$$

where P_t is the transmitting power; G_t and G_r are the antenna gains of the transmitter and the receiver, respectively.

D. Entire hybrid propagation model

For the relatively small-size users, the propagation model inside tunnels can be expressed by:

$$\begin{cases} L_{R_{FS}}, |z_r - z_t| \le l_{free} \\ L_{R_{MW}}, |z_r - z_t| > l_{free} \end{cases} \tag{17}$$

When the distance is smaller than the end point of the free space zone, the propagation is attenuated following the free space model. In the remaining part, it is dominated by multi-mode waveguide mechanism.

The case of the relatively large-size users is more complex. The model structure depends on the relation of the lengths of the near shadowing zone and the free space zone. When $l_{near} < l_{free}$, the model is

$$\begin{cases} L_{R_{NS}}, |z_r - z_t| \le l_{near} \\ L_{R_{FS}}, l_{near} < |z_r - z_t| \le l_{free} \\ L_{R_{MW}}, |z_r - z_t| > l_{free} \end{cases} \tag{18}$$

All the three propagation mechanisms exist. When $l_{near} \ge l_{free}$, the free space propagation is completely replaced by the near shadowing phenomenon:

$$\begin{cases} L_{R_{NS}}, |z_r - z_t| \le l_{near} \\ L_{R_{MW}}, |z_r - z_t| > l_{near} \end{cases} \tag{19}$$

Since there is an interaction between the path loss curves in different zones, the continuity of the predicted path loss can be ensured in the transition between every two zones.

IV. Model Validation

In order to validate the proposed model, two groups of measurements in railway and subway tunnels have been employed.

A. Measurement in railway tunnel

The first set of measurements are carried out in the tunnels on the new high-speed train line from Madrid to Lleida in Spain [9]. According to the test system configuration and environment, following parameters are assigned to the simulation: $f_0 = 900 \times 10^6$, $\lambda = 0.33$, $W = 10.7$, $H = 6.3$, $x_t = 11.43$, $y_t = 3$, $z_t = 0$, $x_r = 8.43$, $y_r = 3$, $\theta = 0.1$, $\gamma = 0.12$, $\varepsilon_v = 5$, $\varepsilon_h = 5$, $\varepsilon_a = 1$, $\sigma_v = 0.01$, $\sigma_h = 0.01$, $\sigma_a = 0$, $\mu_0 = 4\pi \times 10^{-7}$, $\varepsilon_0 = 8.85 \times 10^{-12}$, and the curvature radius of the roof $R = 6.2$.

Fig. 4 shows the comparisons of the received signal power in the measurement and the predicted results of the hybrid propagation model. It can be found that the model accurately predicts the attenuation velocity, the path loss in the free

space propagation zone, the fast fading and the flat fading in the waveguide propagation zone. It is noted that the near shadowing zone is not reflected. This is because the high-speed railway tunnel is very wide and high so that the train is not relatively large in size compared with the railway tunnel. No LOS can be blocked even when the train is passing the transmitter, therefore the near shadowing zone does not exist, but is replaced by the free space propagation zone.

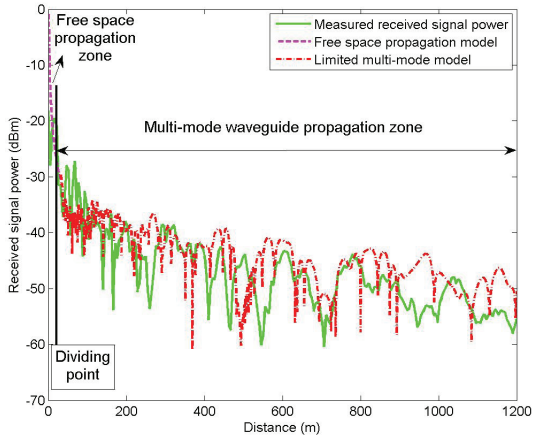

Fig. 4. Comparisons of the received signal power in the measurement carried out in railway tunnel at 900 MHz and the predicted results.

B. Measurement in subway tunnel

The second kind of measurements are performed at 2.4 GHz, for the planning of the CBTC system in the Line 10 tunnels of Madrid's subway [12]. Following parameters are used for the simulation: $f_0 = 2.454 \times 10^9$, $\lambda = 0.125$, $W = 9.8$, $H = 6.2$, $x_t = 0.25$, $y_t = 4$, $z_t = 0$, $x_r = 4$, $y_r = 3.5$, $\theta = 0.22$, $\gamma = 0.2$, $\varepsilon_v = 5$, $\varepsilon_h = 5$, $\varepsilon_a = 1$, $\sigma_v = 0.01$, $\sigma_h = 0.01$, $\sigma_a = 0$, $\mu_0 = 4\pi \times 10^{-7}$, $\varepsilon_0 = 8.85 \times 10^{-12}$.

As shown in Fig. 5, the predicted results and the measured received signal power have good agreement. Since the length of the near shadowing zone is longer than the free space propagation zone, only the near shadowing zone can be observed before the multi-mode waveguide region.

V. Conclusion

This paper presents a novel hybrid model inside tunnels. The model covers three propagation mechanisms for two kinds of users, refining and extending previous single method-based models. To begin with, the coupling of the free space propagation model and the limited multi-mode model prevents the invalidation of the waveguide theory in the adjacent region of the transmitter. Furthermore, the important supplementation of the near shadowing zone makes the model more complete and comprehensive. Last but not least, the model considers two types of users and supports different structures. Hence, it can be flexibly used for various concrete situations.

Two kinds of measurements verify the model. The novel hybrid model gives heuristic explanations of the propagation mechanisms. It can be helpful to gain deeper insight into the propagation inside tunnels as well as the system design.

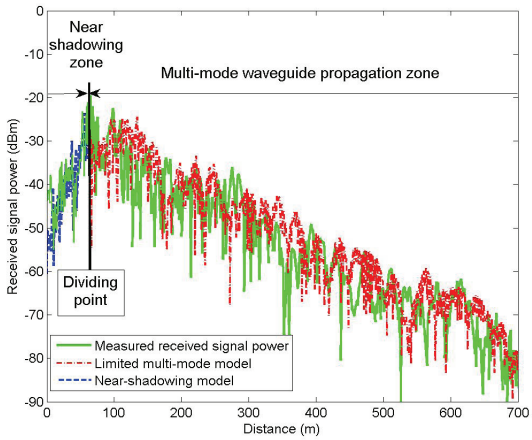

Fig. 5. Comparisons of the received signal power in the measurement carried out in a subway tunnel at 2454 MHz and the predicted results.

References

[1] Y. P. Zhang and Y. Hwang, "Theory of the radio-wave propagation in railway tunnels," *IEEE Trans. Veh. Technol.*, vol. 47, pp. 1027C1036, Aug. 1998.

[2] Y. P. Zhang and H. J. Hong, "Ray-optical modeling of simulcast radio propagation channels in tunnels," *IEEE Trans. Veh. Technol.*, vol. 53, pp. 1800C1808, Nov. 2004.

[3] A. G. Emslie, R. L. Lagace and P. F. Strong, "Theory of the propagation of UHF radio waves in coal mine tunnels," *IEEE Trans. Antennas Propag.*, Vol. 23, pp. 192-205, 1975.

[4] D. G. Dudley, M. Lienar, S. F. Mahmud and P. Degauque, "Wireless propagation in tunnels," *IEEE Antennas Propag. Magazine*, Vol. 49, pp. 11-26, 2007.

[5] Y. P. Zhang, "A hybrid model for propagation loss prediction in tunnels," *Millennium Conf. Ant. and Propag.*, Davos, Switzerland, April 2000.

[6] R. Martelly and R. Janaswamy, "Modeling radio transmission loss in curved, branched and rough-walled tunnels with the ADI-PE method," *IEEE Trans. Antennas Propag.*, Vol. 58, pp. 2037-2045, Jun. 2010.

[7] K. Guan, Z. D. Zhong, B. Ai and C. Briso-Rodriguez, "Measurement and Modeling of Subway Near Shadowing Phenomenon," in *Proc. CHINACOM*, Beijing, 2010, pp. 1-5.

[8] K. Guan, Z. D. Zhong, B. Ai and C. Briso-Rodriguez, "Propagation mechanism analysis before the break point inside tunnels," in *Proc. IEEE 74th Veh. Technol. Conf.*, Sep. 2011, pp. 1-5.

[9] C. Briso-Rodriguez, J. M. Cruz and J. I. Alonso, "Measurements and Modeling of Distributed Antenna Systems in Railway Tunnels," *Veh. Technol., IEEE Trans*, vol. 56, Issue 5, Part 2, pp. 2870-2879, Sept. 2007.

[10] A. Hrovat, G. Kandus and T. Javornik, "Four-slope channel model for path loss prediction in tunnels at 400 MHz," *IET Microwaves, Antennas and Propagation* , Vol. 4, pp. 571-582, Dec. 2010.

[11] S. SAUNDERS, "Antennas and propagation for wireless communication systems," John Wiley and Sons Ltd, Chichester, England, 2005.

[12] K. Guan, Z. D. Zhong, C. Briso-Rodriguez and J. I. Alonso, "Measurement of Distributed Antenna Systems at 2.4 GHz in a Realistic Subway Tunnel Environment," accepted by *IEEE Trans. on Veh. Technol.* , 2011.

[13] Z. Sun and I. F. Akyildiz, "Channel Modeling and Analysis for Wireless Networks in Underground Mines and Road Tunnels," *IEEE Trans. on Communications*, vol. 58, no. 6, pp. 1758-1768, June 2010.

[14] J. M. Molina-Garcia-Pardo, M. Lienard, A. Nasr and P. Degauque, "On the possibility of interpreting field variations and polarization in arched tunnels using a model for propagation in rectangular or circular tunnels," *IEEE Trans. Antenna Propag.*, vol. 56, no. 9, pp. 1206-1211, April 2008.

[15] Y. P. Zhang and Y. Hwang, "Characterization of UHF radio propagation channels in tunnel environments for microcellular and personal communications," *IEEE Trans. Veh. Technol.*, Vol. 47, pp.283-296, 1998.

[16] K. D. Laakmann and W. H. Steier,"Waveguides: characteristic modes of hollow rectangular dielectric waveguides," *Appl. Optics*, vol. 15, no. 5, pp. 1334-1340, May 1976.

[17] Y. P. Zhang and Y. Hwang, "Enhancement of rectangular tunnel waveguide model," *Microwave Conf. Proceedings 1997. APMC '97, 1997 Asia-Pacific*, Vol. 1, pp. 197 - 200, Dec. 1997.